

Antiferromagnetic component due to orbital selective ferromagnetism in $\text{La}_5\text{Co}_2\text{Ge}_3$

Giuseppe Cuono,^{1,*} Carmine Autieri,¹ and Marcin M. Wysocki^{1,†}

¹*International Research Centre MagTop, Institute of Physics, Polish Academy of Sciences,
Aleja Lotników 32/46, PL-02668 Warsaw, Poland*

(Dated: April 30, 2021)

We present density functional theory calculations for low- T_c metallic ferromagnet $\text{La}_5\text{Co}_2\text{Ge}_3$ at ambient and applied pressures. Our investigations reveal that the system is a quasi-one-dimensional ferromagnet with a peculiar coexistence of two different orbital-selective magnetic moments from two crystallographic inequivalent Co1 and Co2 atoms. Namely, due to different crystal-field splitting, the magnetic moment of Co1 atoms predominantly derives from d_{xz} orbital whereas of Co2 atoms from d_{xy} orbital. These two types of atoms develop unequal net magnetic moments, a feature that due to alternating sequence of Co1 and Co2 atoms gives rise to antiferromagnetic component along crystallographic c -direction. Antiferromagnetic component, initially small, drastically increases with applied pressure, until Co2 atoms become nonmagnetic. Our density functional theory results, supported by the analysis of a toy model for the found orbital-selective ferromagnetic order, are consistent with the recently reported resistivity measurements on $\text{La}_5\text{Co}_2\text{Ge}_3$ suggesting the presence of a partially gapped magnetic phase under pressure. Although, proposed here origin of antiferromagnetic component in $\text{La}_5\text{Co}_2\text{Ge}_3$ is an alternative one to the advocated for this material ferromagnetic quantum criticality avoidance, our findings indicate that the effects of the quantum fluctuations can still play a key role at pressure larger than up-to-date measured 5GPa.

I. INTRODUCTION

Low- T_c metallic ferromagnets are systems in which quantum fluctuations can play a key role in understanding of their macroscopic properties when tuned with clean, i.e. not introducing disorder, means such as pressure or magnetic field¹. Namely, it has been theoretically predicted that ferromagnetic quantum critical point (QCP) in these systems is generically avoided and at low temperature a first order transition² or other, likely spatially modulated phases^{3–5} should appear instead. Moreover, quantum-fluctuation driven pressure-magnetic-field-temperature phase diagrams of low- T_c itinerant ferromagnets can have a so-called tricritical wing structure⁶.

Multiple experiments on metallic ferromagnets have shown consistency between measured properties and theoretical expectations relying on avoided QCP scenario. Namely, at low temperatures there have been observed: (i) change from a second to first-order ferromagnet (FM) to paramagnet transition^{7–10}, (ii) emergence of spatially modulated phase^{11–16} and (iii) appearance of tricritical wings^{8–10,14,17–19}. Very recently itinerant ferromagnet $\text{La}_5\text{Co}_2\text{Ge}_3$, that is the focus of the current work, has joined the above list as an example of emergence of the new, potentially spatially modulated, phase out of FM under pressure²⁰.

For the proper description of metallic ferromagnets there has been also proposed a Stoner type of approach based on common among them electronic structure property that is mixing of correlated and uncorrelated bands in the vicinity of the Fermi level. This approach, just as QCP avoidance approach, is able to rationalize observations of first order transition^{21,22}, tricritical wings^{22,23}, and modulated phase²⁴ under pressure. Although more restricted by the material-specific input parameters, this

microscopic approach has an advantage as it captures the appearance of the two distinct FM phases ubiquitous among metallic ferromagnets^{7,8,14,17,25}. Moreover, the approach inspired the proposal of a consistent theory of the superconductivity in UGe_2 .²⁶

Possible ambiguity in the microscopic foundations of generic features among metallic ferromagnets calls for a critical and thorough theoretical investigation of each of the compounds separately in order to provide conclusive interpretation of particular observations. In this light recently reported measurements for low- T_c metallic ferromagnet $\text{La}_5\text{Co}_2\text{Ge}_3$ indicating the appearance of partially gapped, presumably due to emergent antiferromagnetic (AFM) component, high-pressure magnetic phase²⁰, raised a question about the underlying mechanism responsible for this novel state. Therefore, in the current work, by means of density functional theory (DFT) calculations we analyze electronic and magnetic properties of $\text{La}_5\text{Co}_2\text{Ge}_3$ in order to shed light on the origin of this enigmatic high pressure magnetic phase.

Our results confirm that the high pressure, partially gapped magnetic phase in $\text{La}_5\text{Co}_2\text{Ge}_3$ as suggested in Ref. 20 is indeed characterized with a large AFM component. However, the origin of a spatial modulation according to our calculations is attributed to the d -orbital selectivity, stemming from a presence of crystallographically inequivalent cobalt atoms, Co1 and Co2 (see Fig. 1), rather than to purely electronic-like mechanism as in QCP avoidance^{3–5} or correlated-uncorrelated orbitals mixing²⁴ scenarios. We have found that ferromagnetism in $\text{La}_5\text{Co}_2\text{Ge}_3$ due to two different crystal fields on cobalt sites predominantly derives from d_{xz} orbital of Co1 atoms whereas from d_{xy} orbital of Co2 atoms. In consequence, these two types of atoms develop different net magnetic moments, that due to alternation of Co1 and Co2 atoms gives rise to AFM component along c -axis. The ampli-

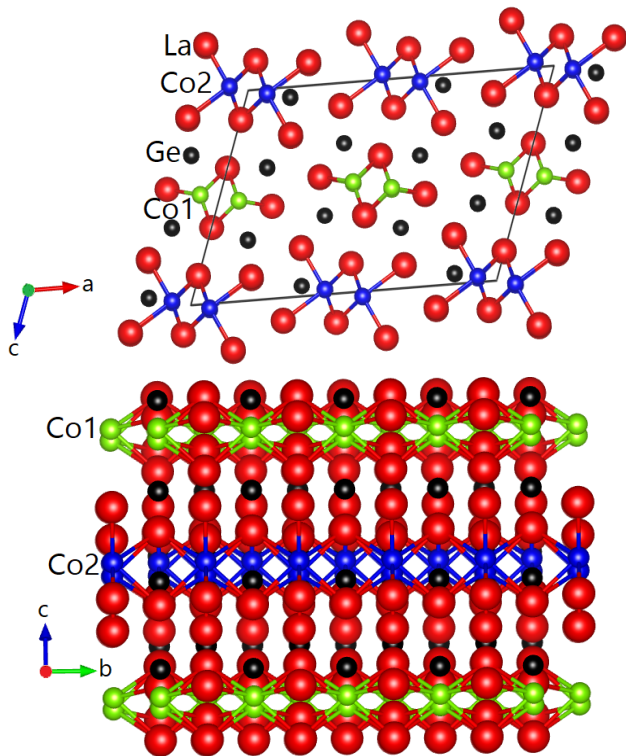


FIG. 1: Crystal structure of $\text{La}_5\text{Co}_2\text{Ge}_3$. Green and blue spheres denote Co1 and Co2 atoms, while red and black spheres La and Ge atoms. Co1 and Co2 atoms form chains along b -direction.

tude of a spatial modulation, at ambient pressure rather small, substantially grows with unit cell contraction, until Co2 atoms becomes nonmagnetic. Analysis of a toy-model capturing the essential character of the found ferromagnetic order with AFM component shows consistency with the resistance measurements for $\text{La}_5\text{Co}_2\text{Ge}_3$ in the high-pressure *new state*²⁰. Although, our results indicate rather minor role played by quantum fluctuation in the interpretation of recent observations in $\text{La}_5\text{Co}_2\text{Ge}_3$, we note that the ferromagnetic quantum criticality avoidance can take place at pressure larger than up-to-date measured 5GPa.

II. COMPUTATIONAL DETAILS

We have performed DFT calculations by using the VASP package^{27–29}. The core and the valence electrons were treated within the Projector Augmented Wave³⁰ method with a cutoff of 400 eV for the plane wave basis. For the relaxation, we have used a revised Perdew-Burke-Ernzerhof for solids (PBEsol)³¹ that improves the equilibrium properties of itinerant magnetic systems^{32–34}. The calculations as a function of the volume were done tuning the total volume but keeping unchanged the ratios between the lattice constants. After relaxation, the Local Density Approximation (LDA) has been used and

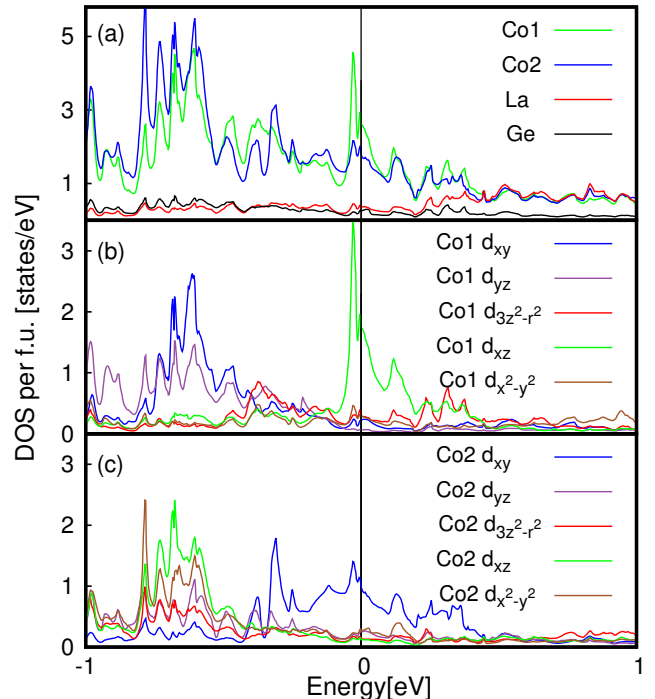


FIG. 2: (a) Nonmagnetic partial densities of states (PDOS) of d -orbitals of Co1 and Co2 atoms and combined PDOS of s , p and d orbitals of La and Ge atoms. The Fermi level is set at the zero energy. (b) The contributions of the d orbitals of Co1 to the nonmagnetic density of states. (c) The contributions of the d orbitals of Co2 to the nonmagnetic density of states.

the Perdew–Zunger³⁵ parametrization of the Ceperly–Alder³⁶ data have been considered. This choice is motivated by the fact that the functional used within PBEsol is the most suited for the relaxation, while the LDA gives a better agreement with the experimental magnetization of magnetic metallic systems. These calculations have been performed using a $2 \times 12 \times 4$ k -point grid, in such a way to have 96 k -points in the first Brillouin zone. For the Brillouin zone integration we have used the tetrahedron method³⁷ in order to get the partial density of states (PDOS) and the magnetic properties of the system.

III. STRUCTURAL AND ELECTRONIC PROPERTIES

The crystal structure of $\text{La}_5\text{Co}_2\text{Ge}_3$ belongs to the $\text{R}_5\text{Co}_2\text{Ge}_3$ family, and the symbol is mS40 ^{38,39}. The y coordinates for all atoms in this structure equal to zero, namely the atoms in this structure are located either on planes at $y = 0$ or $y = 1/2$ arising from the C center in space group C2/m . The crystal structure of $\text{La}_5\text{Co}_2\text{Ge}_3$ is shown in the top panel of Fig. 1. There are two crystallographically inequivalent cobalt atoms Co1 and Co2 forming chains along the b axis, as shown in the bottom

panel of Fig. 1. The lattice constants are $a=18.3540 \text{ \AA}$, $b=4.3479 \text{ \AA}$ and $c=13.2790 \text{ \AA}$.³⁸

Regarding the electronic properties, in Fig. 2(a) we show the partial densities of states for the dominant orbitals in the vicinity of the Fermi level: d orbitals of Co1 and Co2 and combined s , p and d orbitals of La and Ge. The calculation shows no charge transfer, namely there is no oxidation state. Therefore, due to the crystal field the $4s^23d^7$ electronic configuration of the elemental Co moves to $3d^9$. The low energy states can be reduced to the d -states of the d^9 Co atoms, therefore, we can have a maximum magnetic moment of $1 \mu_B/\text{Co}$ (Bohr magneton per Co atom).

Cobalt d -orbital PDOS in Fig. 2(a) as expected for a metallic Stoner ferromagnet provides a large peak at the Fermi level. However, different PDOS at the Fermi level for Co1 and Co2 seen in Fig. 2(a) clearly demonstrate that d orbitals of Co1 and Co2 can lead to spatially nonuniform magnetic properties of the system, i.e. more fragile magnetism of Co2 than of Co1 atoms. In order to have more insight into that feature in Figs. 2(b,c) we plot PDOS contribution from crystal field split d orbitals at Co1 and Co2 atoms respectively. Although all orbitals are mixed, clearly only d_{xz} of Co1 and the d_{xy} of Co2 present a sufficiently large peak at the Fermi level to satisfy Stoner criterion. For that reason these two orbitals are predominantly responsible for the formation of a ferromagnetic state in $\text{La}_5\text{Co}_2\text{Ge}_3$.

IV. MAGNETIC PROPERTIES

In this Section, we analyze the magnetic properties of $\text{La}_5\text{Co}_2\text{Ge}_3$ at ambient and applied pressure. Magnetism in this system derives solely from $3d$ orbitals of cobalt, due to a marginal contribution of other orbitals at the Fermi level (cf. Fig. 2(a)). Moreover, magnetic properties of Co1 and Co2 atoms are expected to be different due to their different d -orbital composition near Fermi level (cf. Fig 2(b,c)). Therefore, in the following we focus only on the magnetism of Co1 and Co2 atoms.

First, we find that at ambient pressure the magnetic coupling among cobalt atoms within the chain along b -axis is robustly ferromagnetic and is much stronger than this between neighbouring chains, irrespectively whether encompassing Co1 or Co2 sites. Next, by testing different magnetic configurations in the a - c plane for the neighbouring chains, we have established that interchain couplings, though weaker due to large atomic distances, are also robustly ferromagnetic. The difference to the closest higher energy state with antiferromagnetic interchain correlations is around 2.3 meV . The magnetic moments obtained at ambient pressure with the experimental atomic positions are $0.486\mu_B$ at Co1 and $0.381\mu_B$ at Co2 atoms. Their inequality is expected due to different d -orbital contribution in the vicinity of the Fermi level as demonstrated in the nonmagnetic PDOS in Fig. 2. These values are higher than the experimentally de-

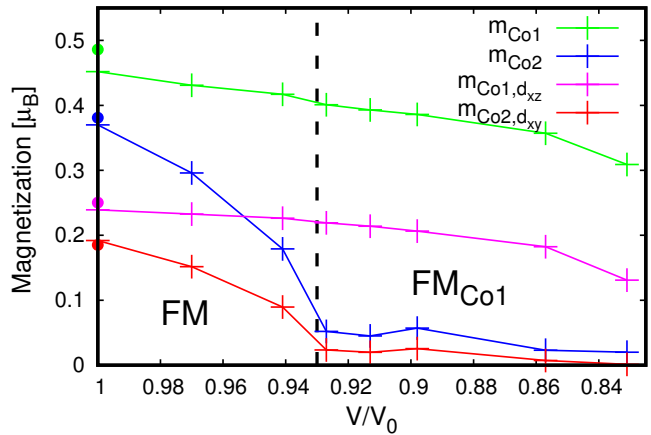


FIG. 3: Magnetic moments of Co1 and Co2 as a function of decreasing primitive cell volume V/V_0 , where V_0 is the experimental volume at ambient pressure. The green and blue lines indicate the evolution of magnetic moments at Co1 and Co2 atoms respectively. We have also included magnetic moments of the dominant d -orbitals, d_{xz} of Co1 (magenta line) and d_{xy} of Co2 (red line) atoms. Magnetic moments marked with cross are obtained with relaxation procedure whereas those marked with a dot are obtained at experimental ambient pressure volume³⁸.

termined magnetic moment $0.1 \mu_B$ in $\text{La}_5\text{Co}_2\text{Ge}_3$ ²⁰ as happens also in other DFT calculations of low magnetic moment ferromagnets.

Due to the weak interchain magnetic coupling $\text{La}_5\text{Co}_2\text{Ge}_3$ is a quasi-one-dimensional ferromagnet with extremely low T_C . We note, that in the same manner as for other recently discovered quasi-one-dimensional compounds^{40–44}, in $\text{La}_5\text{Co}_2\text{Ge}_3$ weak interchain magnetic coupling is critical for the stabilization of long-range magnetic order in the context of the Mermin-Wagner theorem⁴⁵.

Next, we analyze the magnetic properties of our system under applied pressure. To simulate the effect of the external pressure acting on the system, we have performed our calculations at different values of the volume of the primitive cell, V/V_0 where V_0 is the experimental volume at ambient pressure³⁸. As experimental atomic positions are not known for $\text{La}_5\text{Co}_2\text{Ge}_3$ under pressure to access magnetic properties for contracted volumes we perform the structural relaxation. Such approach is sensible in light of found good agreement between magnetic moments of Co1 and Co2 (cf. Fig. 3) at ambient pressure obtained for the experimental position and the structural relaxed structure.

Applied pressure brings the atoms closer simply increasing the hopping parameters between Co atom, enlarging the electronic bandwidth. Such procedure as a rule reduces the magnetic moment in itinerant magnetic systems⁴⁶. In Fig. 3 we present the evolution of magnetic moments on Co1 and Co2 atoms with decreasing unit

cell volume that follows this expectation. However, both types of atoms react in a contrasting manner to applied pressure. Namely, the magnetization of the Co2 rapidly drops at $V/V_0 \approx 0.93$ and Co2 atoms become nonmagnetic, while the magnetization of the Co1 at least for $V/V_0 \gtrsim 0.83$ is rather weakly decreasing. We note that nonzero magnetization on Co2 atoms for $V/V_0 \lesssim 0.93$ is just an effect of coupling to Co1 chains and long-range character of magnetic order.

In Fig. 3 we have included evolution with applied pressure of magnetic moments solely from orbitals dominant at ambient pressure (cf. Fig. 2), i.e. d_{xz} of the Co1 atoms and d_{xy} of Co2 atoms. These orbitals provide as much as half of the total magnetization on respective cobalt atoms, confirming their leading role in determining magnetic properties of $\text{La}_5\text{Co}_2\text{Ge}_3$ also at applied pressure. In result we firmly establish that the reason for the contrasting magnetization evolution on the two types of Co atoms under pressure is that different orbitals drive the magnetism on crystallographically distinct cobalt sites.

The magnetization difference present even at ambient pressure follows that magnetic state in $\text{La}_5\text{Co}_2\text{Ge}_3$ has antiferromagnetic component along c axis due to alternation of Co1 and Co2 chains (cf. Fig. 1). Difference between magnetic moments between Co1 and Co2, at ambient pressure rather small, drastically increases with the unit cell contraction until Co2 atoms become nonmagnetic, for $V/V_0 \lesssim 0.93$. Then the magnetization difference stays large because of the weak decrease of magnetization on Co1 atoms in response to applied pressure. Such spatial modulation, as we will discuss in more detail in the next Section produces a partial gapping of the Fermi surface what is consistent with the experimental observations under pressure²⁰. Although, according to our calculations gapping is also present at ambient pressure, AFM component is then small and likely hindered in resistivity spectra due to various sources of disorder and scattering process. On the other hand, once Co2 chains become nonmagnetic AFM component is large and likely only then gives rise to a well pronounced hump in resistivity spectra.

Therefore, we suggest that recently reported ferromagnetic to *new state* transition under pressure²⁰ is in fact crossover within the same ferromagnetic phase with the *new state* being region characterized just with a larger AFM component. In that manner, we also suggest that the *new state* region is characterized by nonmagnetic Co2 chains (FM_{Co1} in Fig. 3), where spatial alteration of magnetization is the largest.

In the next Section we propose a toy model that is designed to mimic magnetic order of $\text{La}_5\text{Co}_2\text{Ge}_3$ along c -axis in FM_{Co1} region (cf. Fig. 3). Transport characteristics obtained for this model additionally supports consistency of our DFT results with recent measurements for $\text{La}_5\text{Co}_2\text{Ge}_3$ ²⁰.

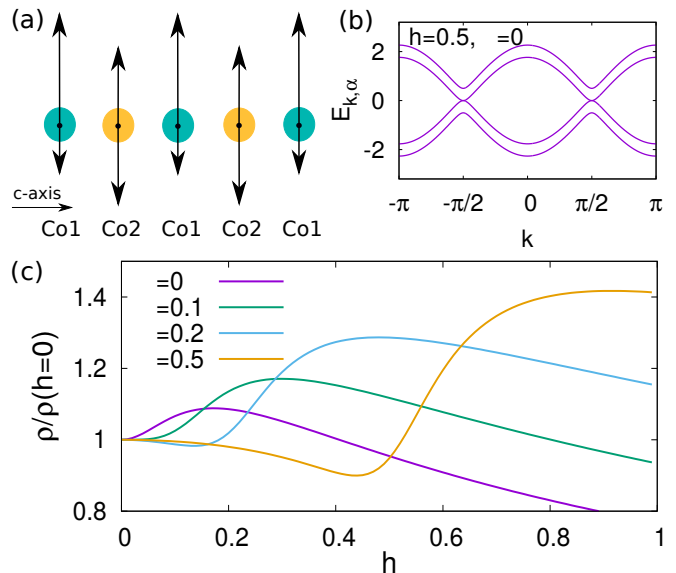


FIG. 4: (a) Schematic cartoon of alternating magnetic/non-magnetic cobalt sites along c -axis (arrows denote up and down spin population) visualizing peculiar magnetic behavior of $\text{La}_5\text{Co}_2\text{Ge}_3$ under applied pressure (FM_{Co1} phase). (b) Partially gapped spectrum of the toy model capturing features of magnetic order visualized in (a), where h is Zeeman splitting on Co1 sites and μ chemical potential. (c) Normalized resistance as a function of Zeeman splitting h on Co1 sites for selected values of chemical potential μ .

V. TOY MODEL

Orbital selective ferromagnetism in $\text{La}_5\text{Co}_2\text{Ge}_3$ predominantly relies on a distinct behavior of two d -orbitals yielding different magnetic moments on Co1 and Co2 sites. On the phenomenological ground, a single-orbital model with a site dependent Zeeman field can mimic the same magnetic order. We found that the analysis of such artificial system is instructive in the interpretation of the recent resistance measurements in $\text{La}_5\text{Co}_2\text{Ge}_3$ along c -axis²⁰. Therefore, in the following we analyze one-dimensional toy model capturing character of magnetic order FM_{Co1} of $\text{La}_5\text{Co}_2\text{Ge}_3$ along c -axis (schematically drawn in Fig. 4(a)), thus with a Zeeman field, h present only on Co1 sites, and described by Hamiltonian

$$H = \sum_{k\sigma} (\epsilon_k - \mu) c_{k\sigma}^\dagger c_{k\sigma} - \sum_{i \in \text{Co1}, \sigma} \sigma h c_{i\sigma}^\dagger c_{i\sigma} \quad (1)$$

where $c_k^{(\dagger)}$ and $c_i^{(\dagger)}$ are annihilation (creation) operators in the momentum and real space respectively. Here, μ is global chemical potential, $\sigma = \pm$ and relation dispersion $\epsilon_k = -2t \cos k$ is assumed to be generated by the hopping t between nearest Co1 and Co2 sites which is set as an energy unit $t = 1$. We note that in principle t is very small due to large distance between neighbouring cobalt atoms along c -axis.

With the help of the above toy model we aim to show that FM_{Co1} phase is consistent with resistance upturn

with lowering the temperature measured for $\text{La}_5\text{Co}_2\text{Ge}_3$ in *new state*²⁰. First, we notice that lowering temperature below $T_C \simeq 7\text{K}$ for $\text{La}_5\text{Co}_2\text{Ge}_3$ in the *new state* in the first approximation can be captured by the increase of the magnetic moment solely on Co1 atoms. In the proposed toy model this translates to an increase of field h . Therefore in the following we will show that increasing h can lead to the increase in the resistance in the qualitative agreement with observations for $\text{La}_5\text{Co}_2\text{Ge}_3$ in the *new state*²⁰.

Fourier transform of site-dependent Zeeman splitting leads to Hamiltonian in reduced Brillouin zone (RBZ) that explicitly describes the coexistence of ferromagnetic and antiferromagnetic orders,

$$H = \sum_{k \in \text{RBZ}, \sigma} \Psi_{k\sigma}^\dagger \begin{pmatrix} \epsilon_k - \mu - \frac{\sigma h}{2} & -\frac{\sigma h}{2} \\ -\frac{\sigma h}{2} & -\epsilon_k - \mu - \frac{\sigma h}{2} \end{pmatrix} \Psi_{k\sigma}, \quad (2)$$

where $\Psi_{k\sigma}^\dagger \equiv \{c_{k\sigma}^\dagger, c_{k+\pi\sigma}^\dagger\}$. The spectrum of the Hamiltonian consists of four eigenvalues $E_{k,\alpha \in \{1-4\}} = \pm \frac{h}{2} - \mu \pm \sqrt{(\frac{h}{2})^2 + \epsilon_k^2}$. This spectrum once h is nonzero is partially gapped due to antiferromagnetic component (cf. Fig. 4(b)) and thus can account for an increase of resistance with increasing h . In order to explicitly visualize that statement we calculate coherent conductance at zero temperature with respect to increasing h with the above toy model's spectrum using Landauer formula,

$$G = \frac{dI}{dV} = \frac{e^2}{h} T(0) \quad (3)$$

where transmission function T is related to spectral function of the model and can be approximated as

$$T(E) = \sum_{k\alpha} \frac{1}{\pi} \frac{\Gamma}{(E - E_{k\alpha})^2 + \Gamma^2}. \quad (4)$$

Here factor Γ broadens spectral function in order to account for a realistic nature of the system encompassing various sources of disorder and scattering processes, and we assume $\Gamma = 0.1$. In Figure 4(c) we plot resistance, $\rho = 1/G$ as a function of Zeeman splitting h for selected values of global chemical potential, and normalized to $\rho(h = 0)$. Dependently on the chemical potential resistance shows increase either immediately with emergence of magnetism (small $|\mu|$) or for larger fields h (large $|\mu|$). Absolute value appears as toy model is symmetric with respect to $\mu = 0$, what means that resistance curves are the same for $\pm\mu$.

VI. SUMMARY

We study electronic and magnetic properties of metallic low- T_C ferromagnet $\text{La}_5\text{Co}_2\text{Ge}_3$ at ambient and applied pressure by means of density functional calculations. We establish that $\text{La}_5\text{Co}_2\text{Ge}_3$ is quasi-one-dimensional orbital selective ferromagnet. Namely, two different d orbitals are magnetically active on two crystallographically inequivalent cobalt sites Co1 and Co2. This results in drastically different evolution of magnetic moments on each type of atoms in response to applied pressure. Namely Co2 atoms for relatively small unit cell contraction become nonmagnetic in sharp contrast to rather robust ferromagnetism of Co1 atoms. The alternating sequence of Co1 and Co2 atoms along c axis providing spatial modulation of magnetization gives rise to a sizable antiferromagnetic component on top of ferromagnetic state.

In that manner we confirm that recently observed enigmatic partially gapped high pressure phase in $\text{La}_5\text{Co}_2\text{Ge}_3$ ²⁰ is indeed related to antiferromagnetic component. However, there is a crossover rather than phase transition with applied pressure, as the ambient pressure phase has also a small AFM component. Our calculations indicate orbital selectivity rather than quantum critical avoidance as a driving mechanism for the presence of sizable AFM component under pressure in $\text{La}_5\text{Co}_2\text{Ge}_3$. We note that effects related to quantum fluctuation² can be still of critical importance at larger than up to date measured (5GPa) pressures where ferromagnetism of Co1 would go down towards zero temperature.

Acknowledgments

The work is supported by the Foundation for Polish Science through the International Research Agendas program co-financed by the European Union within the Smart Growth Operational Programme. We acknowledge the access to the computing facilities of the Interdisciplinary Center of Modeling at the University of Warsaw, Grants No. G75-10, G84-0, GB84-1 and GB84-7. We acknowledge the CINECA award under the ISCRA initiatives IsC81 "DISTANCE" and IsC85 "TOPMOST" Grant, for the availability of high-performance computing resources and support.

* Electronic address: gcuono@magtop.ifpan.edu.pl

† Electronic address: wysokinski@magtop.ifpan.edu.pl

¹ M. Brando, D. Belitz, F. M. Grosche, and T. R. Kirkpatrick, *Rev. Mod. Phys.* **88**, 025006 (2016).

² D. Belitz, T. R. Kirkpatrick, and T. Vojta, *Phys. Rev. B*

55, 9452 (1997).

³ A. V. Chubukov, C. Pépin, and J. Rech, *Phys. Rev. Lett.* **92**, 147003 (2004).

⁴ G. J. Conduit, A. G. Green, and B. D. Simons, *Phys. Rev. Lett.* **103**, 207201 (2009).

- ⁵ U. Karahasanovic, F. Krüger, and A. G. Green, *Phys. Rev. B* **85**, 165111 (2012).
- ⁶ D. Belitz, T. R. Kirkpatrick, and J. Rollbühler, *Phys. Rev. Lett.* **94**, 247205 (2005).
- ⁷ C. Pfeleiderer and A. D. Huxley, *Phys. Rev. Lett.* **89**, 147005 (2002).
- ⁸ M. Uhlarz, C. Pfeleiderer, and S. M. Hayden, *Phys. Rev. Lett.* **93**, 256404 (2004).
- ⁹ S. Araki, M. Hayashida, N. Nishiumi, H. Manabe, Y. Ikeda, T. C. Kobayashi, K. Murata, Y. Inada, P. Wiśniewski, D. Aoki, et al., *J. Phys. Soc. Jpn.* **84**, 024705 (2015).
- ¹⁰ Y. Shimizu, D. Braithwaite, B. Salce, T. Combier, D. Aoki, E. N. Hering, S. M. Ramos, and J. Flouquet, *Phys. Rev. B* **91**, 125115 (2015), URL <https://link.aps.org/doi/10.1103/PhysRevB.91.125115>.
- ¹¹ V. A. Sidorov, E. D. Bauer, N. A. Frederick, J. R. Jeffries, S. Nakatsuji, N. O. Moreno, J. D. Thompson, M. B. Maple, and Z. Fisk, *Phys. Rev. B* **67**, 224419 (2003).
- ¹² H. Kotegawa, T. Toyama, S. Kitagawa, H. Tou, R. Yamauchi, E. Matsuoka, and H. Sugawara, *J. Phys. Soc. Jap.* **82**, 123711 (2013).
- ¹³ V. Taufour, U. S. Kaluarachchi, R. Khasanov, M. C. Nguyen, Z. Guguchia, P. K. Biswas, P. Bonfà, R. De Renzi, X. Lin, S. K. Kim, et al., *Phys. Rev. Lett.* **117**, 037207 (2016).
- ¹⁴ U. S. Kaluarachchi, S. L. Bud'ko, P. C. Canfield, and V. Taufour, *Nat. Comm.* **8**, 546 (2017).
- ¹⁵ U. S. Kaluarachchi, V. Taufour, S. L. Bud'ko, and P. C. Canfield, *Phys. Rev. B* **97**, 045139 (2018).
- ¹⁶ E. Gati, J. M. Wilde, R. Khasanov, L. Xiang, S. Dissanayake, R. Gupta, M. Matsuda, F. Ye, B. Haberl, U. Kaluarachchi, et al., *Phys. Rev. B* **103**, 075111 (2021), URL <https://link.aps.org/doi/10.1103/PhysRevB.103.075111>.
- ¹⁷ V. Taufour, D. Aoki, G. Knebel, and J. Flouquet, *Phys. Rev. Lett.* **105**, 217201 (2010).
- ¹⁸ H. Kotegawa, V. Taufour, D. Aoki, G. Knebel, and J. Flouquet, *J. Phys. Soc. Jpn.* **80**, 083703 (2011).
- ¹⁹ D. Aoki, T. Combier, V. Taufour, T. D. Matsuda, G. Knebel, H. Kotegawa, and J. Flouquet, *Journal of the Physical Society of Japan* **80**, 094711 (2011), <https://doi.org/10.1143/JPSJ.80.094711>, URL <https://doi.org/10.1143/JPSJ.80.094711>.
- ²⁰ L. Xiang, E. Gati, S. L. Bud'ko, S. M. Saunders, and P. C. Canfield, *Phys. Rev. B* **103**, 054419 (2021), URL <https://link.aps.org/doi/10.1103/PhysRevB.103.054419>.
- ²¹ M. M. Wysokiński, M. Abram, and J. Spalek, *Phys. Rev. B* **90**, 081114(R) (2014).
- ²² M. M. Wysokiński, M. Abram, and J. Spalek, *Phys. Rev. B* **91**, 081108(R) (2015).
- ²³ M. Abram, M. M. Wysokiński, and J. Spalek, *J. Mag. Mag. Mat.* **400**, 27 (2016).
- ²⁴ M. M. Wysokiński, *Scientific Reports* **9**, 19461 (2019), URL <https://doi.org/10.1038/s41598-019-55658-x>.
- ²⁵ T. C. Kobayashi, H. Hidaka, T. Fujiwara, M. Tanaka, K. Takeda, T. Akazawa, K. Shimizu, S. Kirita, R. Asai, H. Nakawaki, et al., *J. Phys.: Condens. Matter* **19**, 125205 (2007).
- ²⁶ E. Kądziaława-Major, M. Fidrysiak, P. Kubiczek, and J. Spalek, *Phys. Rev. B* **97**, 224519 (2018).
- ²⁷ G. Kresse and J. Hafner, *Phys. Rev. B* **47**, 558 (1993), URL <https://link.aps.org/doi/10.1103/PhysRevB.47.558>.
- ²⁸ G. Kresse and J. Furthmüller, *Computational Materials Science* **6**, 15 (1996), ISSN 0927-0256, URL <https://www.sciencedirect.com/science/article/pii/S0927025696000080>.
- ²⁹ G. Kresse and J. Furthmüller, *Phys. Rev. B* **54**, 11169 (1996), URL <https://link.aps.org/doi/10.1103/PhysRevB.54.11169>.
- ³⁰ G. Kresse and D. Joubert, *Phys. Rev. B* **59**, 1758 (1999), URL <https://link.aps.org/doi/10.1103/PhysRevB.59.1758>.
- ³¹ J. P. Perdew, A. Ruzsinszky, G. I. Csonka, O. A. Vydrov, G. E. Scuseria, L. A. Constantin, X. Zhou, and K. Burke, *Phys. Rev. Lett.* **100**, 136406 (2008), URL <https://link.aps.org/doi/10.1103/PhysRevLett.100.136406>.
- ³² N. Manca, D. J. Groenendijk, I. Pallecchi, C. Autieri, L. M. K. Tang, F. Telesio, G. Mattoni, A. McCollam, S. Picozzi, and A. D. Caviglia, *Phys. Rev. B* **97**, 081105 (2018), URL <https://link.aps.org/doi/10.1103/PhysRevB.97.081105>.
- ³³ C. Autieri, **28**, 426004 (2016), URL <https://doi.org/10.1088/0953-8984/28/42/426004>.
- ³⁴ C. Autieri and C. Noce, *Philosophical Magazine* **97**, 3276 (2017), URL <https://doi.org/10.1080/14786435.2017.1375607>.
- ³⁵ J. P. Perdew and A. Zunger, *Phys. Rev. B* **23**, 5048 (1981), URL <https://link.aps.org/doi/10.1103/PhysRevB.23.5048>.
- ³⁶ D. M. Ceperley and B. J. Alder, *Phys. Rev. Lett.* **45**, 566 (1980), URL <https://link.aps.org/doi/10.1103/PhysRevLett.45.566>.
- ³⁷ P. E. Blöchl, O. Jepsen, and O. K. Andersen, *Phys. Rev. B* **49**, 16223 (1994), URL <https://link.aps.org/doi/10.1103/PhysRevB.49.16223>.
- ³⁸ S. M. Saunders, L. Xiang, R. Khasanov, T. Kong, Q. Lin, S. L. Bud'ko, and P. C. Canfield, *Phys. Rev. B* **101**, 214405 (2020), URL <https://link.aps.org/doi/10.1103/PhysRevB.101.214405>.
- ³⁹ Q. Lin, K. Aguirre, S. M. Saunders, T. A. Hackett, Y. Liu, V. Taufour, D. Paudyal, S. Budko, P. C. Canfield, and G. J. Miller, *Chemistry – A European Journal* **23**, 10516 (2017), <https://chemistry-europe.onlinelibrary.wiley.com/doi/pdf/10.1002/chem.201702798>, URL <https://chemistry-europe.onlinelibrary.wiley.com/doi/abs/10.1002/chem.201702798>.
- ⁴⁰ G. Cuono, C. Autieri, F. Forte, M. T. Mercaldo, A. Romano, A. Avella, and C. Noce, **21**, 063027 (2019), URL <https://doi.org/10.1088/1367-2630/ab2489>.
- ⁴¹ G. Cuono, C. Autieri, F. Forte, G. Busiello, M. T. Mercaldo, A. Romano, C. Noce, and A. Avella, *AIP Advances* **8**, 101312 (2018).
- ⁴² G. Cuono, F. Forte, A. Romano, X. Ming, J. Luo, C. Autieri, and C. Noce, *Intra-chain collinear magnetism and inter-chain magnetic phases in cr3as3-k-based materials* (2021), 2007.06337.
- ⁴³ G. Cuono, F. Forte, A. Romano, X. Ming, J. Luo, C. Autieri, and C. Noce, *Tuning interchain ferromagnetic instability in a2cr3as3 ternary arsenides by chemical pressure and uniaxial strain* (2021), 2008.03552.
- ⁴⁴ X. Ming, X. Wan, C. Autieri, J. Wen, and X. Zheng, *Phys. Rev. B* **98**, 245123 (2018), URL <https://link.aps.org/doi/10.1103/PhysRevB.98.245123>.
- ⁴⁵ A. Gelfert and W. Nolting, *Journal of Physics: Condensed Matter* **13**, R505 (2001), URL <https://doi.org/10.1088/0953-8984/13/27/201>.
- ⁴⁶ C. Autieri, G. Cuono, F. Forte, and C. Noce, *Journal*

of Physics: Conference Series **969**, 012106 (2018), URL
<https://doi.org/10.1088/1742-6596/969/1/012106>.